STEM CELLS®

TISSUE-SPECIFIC STEM CELLS

# Single Cell Phenotyping Reveals Heterogeneity Among Hematopoietic Stem Cells Following Infection

ADAM L. MACLEAN,[a*] MAIA A. SMITH,[a*] JULIANE LIEPE,[a] AARON SIM,[a] REEMA KHORSHED,[a] NARGES M. RASHIDI,[a] NICO SCHERF,[b] AXEL KRINNER,[b] INGO ROEDER,[b] CRISTINA LO CELSO,[a] MICHAEL P. H. STUMPF [a,c]

[a]Department of Life Sciences, Imperial College London, London, United Kingdom; [b]Institute for Medical Informatics and Biometry, Technische Universitat Dresden, Dresden, Germany; [c]MRC London Institute of Medical Sciences, Imperial College London, London, United Kingdom

*Co-first authors.

Correspondence: Adam L. MacLean, Ph.D., Department of Life Sciences, Imperial College London, London, United Kingdom. Telephone: +442075945114; e-mail: a.maclean@uci.edu; or Michael P. H. Stumpf, Department of Life Sciences, Imperial College London, London, United Kingdom. Telephone: +442075945114; e-mail: m.stumpf@imperial.ac.uk

Received October 24, 2016; accepted for publication June 1, 2017; first published online in STEM CELLS *EXPRESS* August 22, 2017.

http://dx.doi.org/10.1002/stem.2692



This article was published online on 24 September 2017. Author Contribution information was incomplete. This notice is included in the online and print versions to indicate that both have been corrected 29 September 2017.

**Key Words.** In vivo systems biology • Cell migration • Bone marrow • Mathematical modeling • In vivo tracking • Stem cell-microenvironment interactions

## ABSTRACT

**The hematopoietic stem cell (HSC) niche provides essential microenvironmental cues for the production and maintenance of HSCs within the bone marrow. During inflammation, hematopoietic dynamics are perturbed, but it is not known whether changes to the HSC–niche interaction occur as a result. We visualize HSCs directly in vivo, enabling detailed analysis of the 3D niche dynamics and migration patterns in murine bone marrow following *Trichinella spiralis* infection. Spatial statistical analysis of these HSC trajectories reveals two distinct modes of HSC behavior: (a) a pattern of revisiting previously explored space and (b) a pattern of exploring new space. Whereas HSCs from control donors predominantly follow pattern (a), those from infected mice adopt both strategies. Using detailed computational analyses of cell migration tracks and life-history theory, we show that the increased motility of HSCs following infection can, perhaps counterintuitively, enable mice to cope better in deteriorating HSC–niche microenvironments following infection.** STEM CELLS *2017;35:2292–2304*

## SIGNIFICANCE STATEMENT

This analysis shows differences in the migration behavior of hematopoietic stem cells (HSCs) following exposure to infection by *Trichinella spiralis*. HSCs harvested from infected mice show pronounced heterogeneity in their behavior compared with HSCs from healthy mice, in a way that suggests long-lasting agitation following deterioration of the HSC niche environment.

## INTRODUCTION

Hematopoietic stem cell (HSC) function is essential for the development and maintenance of the hematopoietic system [1, 2]. It relies on both cell-intrinsic and cell-extrinsic factors and their interplay at the sites of hematopoiesis [3, 4]. At the sites where hematopoiesis takes place—in adult mammals this is typically the bone marrow, and on occasion the spleen—it is believed that there exist stem cell niches; this term refers to the anatomical and functional influence on HSCs from cell-extrinsic factors. HSC niches have been extensively studied, and an increasingly complex picture is emerging of the stromal and hematopoietic cell types able to influence HSC function, and the molecular cross-talk between HSCs and neighboring cells [5–10]. Nevertheless, there are a host of direct and indirect lines of evidence that point to the existence of dedicated environments that enable, and are indeed crucial for, HSCs to carry out their function.

Vasculature, endothelial, and mesenchymal stromal cells are all constituent members of the stem cell niche, and interact with HSCs via signaling mediated by cytokines including CXCL12 (stromal cell-derived factor) and stem cell factor [3, 11–16]. HSCs have been found to locate near both the arterioles in the area of endosteum, and the smaller sinusoidal capillary vessels that pervade the inner bone marrow cavity [7, 9, 10, 17, 18]. Although the extent of influence of osteoblastic cells (residing near the endosteum) has been contested, they are likely either a constituent of the niche or support the establishment of niches [19]. Resolving this spatial complexity and the cellular dynamics, requires in vivo spatiotemporal data at the level of single HSCs, including ideally also genomic/transcriptomic analysis; but

simultaneous in vivo phenotyping (through live imaging) and molecular characterization of cells currently remains beyond our grasp. A number of relevant studies have helped to reveal homeostatic and nonhomeostatic HSC–niche behavior [20–22]. Spatial data that describe cell migration patterns enable the testing of hypotheses regarding the relative locations of different cell types, the modes of cell movement, and the factors that determine the behavior of migrating cells [23, 24].

Resolving HSC–niche dynamics requires spatiotemporal data not only for homeostatic conditions but also under perturbations. Infection directly perturbs cells of the hematopoietic system through the immune response and, in addition, has recently been shown to directly affect undifferentiated hematopoietic stem and progenitor cells [25–28]. Thus, it provides a suitable model that compliments other HSC perturbations (such as cancer [29] or ageing [10, 30]). There are a host of important reasons for studying the effects of infection on hematopoiesis: many infections, in particular those with high morbidity profoundly affect the constituency of the blood, and for several diseases, an ensuing weakness of the immune response can have the most pronounced medium and long-term consequences for the health of the infected individual. Also for acute, but especially for chronic infections, we lack detailed insights into the mechanisms by which the infection affects the hematopoietic system; although the fact that the HSCs, at the top of the hematopoietic cascade, can be affected is beyond doubt. *How* HSCs respond to a challenge by an infectious agent, and whether they do so uniformly and deterministically, is at best partially understood.

The nematode *Trichinella spiralis* causes trichinosis, a nonlethal infection in mice following ingestion [31]. Parasitic larvae produced in the host migrate to the circulatory system causing initial tissue damage and inflammation that provokes a response from regulatory cytokines following the acute disease phase [32]. This in turn affects hematopoiesis in terms of number and frequency of heaematopoietic progenitors and increases the engraftment ability of HSCs despite their numbers and cell cycle profiles remaining unchanged [21]. This was linked to changes in the behavior of engrafting HSCs [21].

While the importance of single cell molecular profiling is being widely recognized, it is also important to understand the *phenotypic* variability—here of HSC migration behavior—at the single cell level. Here, we characterize and quantify the changes in HSC–niche interactions triggered by infection, at the single cell level. Based on the results of ref. [21]—capturing cell movement via 3D tracking—we subject these imaging data to detailed statistical analysis of the observed movement patterns. We reconstruct the trajectories of HSCs through the bone marrow space and find significant differences between HSCs from control and *Trichinella*-infected mice. Strikingly, HSCs from infected mice show higher levels of sustained migration as well as more pronounced cell-to-cell variability in migration behavior than HSCs from control mice. Taken together, these data show that infection leads to greater heterogeneity in the behavior of HSCs: a subpopulation of HSCs are likely to leave their current niche and explore larger regions of bone marrow space. Within the framework of life history theory [33, 34], we are able to give conditions under which such migration of HSCs may benefit an individual by corresponding to a simple bet-hedging strategy [35, 36], which enables HSCs to move from deteriorating niches into other, more supportive niches. Thus, phenotypic heterogeneity among a stem cell population may be more than just a stochastic phenomenon, but could be a robust strategy [37] that is evolutionary favored. Correspondingly, understanding the cellular responses requires the consideration of individual cells, from which we obtain information on the diversity of the phenotypic response.

## Materials and Methods

### *T. Spiralis* Infection and In Vivo Imaging

Lethally irradiated Col2.3GFP mice were injected with approximately 10,000 DiD labeled LT-HSCs ($Lin^{low}$, *c*-$Kit^{+}$, $Sca1^{+}$, $CD34^{-}$, $Flk2^{-}$), harvested from the bone marrow of either *T. spiralis*-infected wild type mice or age-matched controls 14 days post-infection (Fig. 1). Sixteen hours post-injection, mouse calvarium was imaged in vivo using multiphoton microscopy, capturing hematopoietic stem cells (HSCs), vasculature, and osteoblasts every 5 minutes for 5 hours. For full details see ref. [21].

### Cell Tracking in 3D

Each imaged calvarium contained markers for HSCs, vasculature, and osteoblasts. HSCs were tracked in ImageJ/Fiji [38], using the *TrackMate* plugin, with parameters (estimated diameter, maximum linking distance) set individually for HSCs based on visual inspection of the track, to acquire optimal tracking performance in 3D. HSCs were filtered according to three criteria: roundness, size ($<$15 $\mu$ in diameter), and composition (single-bodied, i.e., not dispersed DiD objects). Following this filtering process, 26 tracks for infected HSCs and 16 tracks for controls HSCs were retained. Figure 2 shows snapshot images taken from the movie data for a healthy control (A) or during infection (B), alongside (C) the resulting tracks projected into 2D (for visualization).

### Construction of $\alpha$-Shapes

To represent the niche space occupied by an HSC, we create an $\alpha$-shape modeled on its 3D track [39, 40]. The HSC is assumed to have a radius of 4 $\mu$m: each 3D coordinate is thus considered to be a sphere of radius 4 $\mu$m. Where step lengths were $>$4/3 $\mu$m apart, a cylinder of radius 4 $\mu$m was created to connect the spheres. To prevent holes in the $\alpha$-shape, inner spheres and cylinders of radius 2 $\mu$m were placed within the 4 $\mu$m spheres and cylinders. Each inner and outer sphere and cylinder was approximated by a set of 500 points sampled from their surface. The R package *alphashape3d* was used to produce the final $\alpha$-shape objects for each HSC. Figure 3A demonstrates the process of $\alpha$-shape construction for a track composed of two steps. Cumulative $\alpha$-shapes were created by repeating the process of $\alpha$-shape construction sequentially, for each successive time point in the HSC track. In Supporting Information Figure S1C, the convex hull of the track used in Supporting Information Figure S1A is shown to illustrate the advantage that $\alpha$-shapes have over convex hulls: they represent both the convexity and the concavity of the shape.

### Curvature Quantification

To quantify the curvature of an $\alpha$-shape, we adapted methods developed for the analysis of protein surface shape [41].

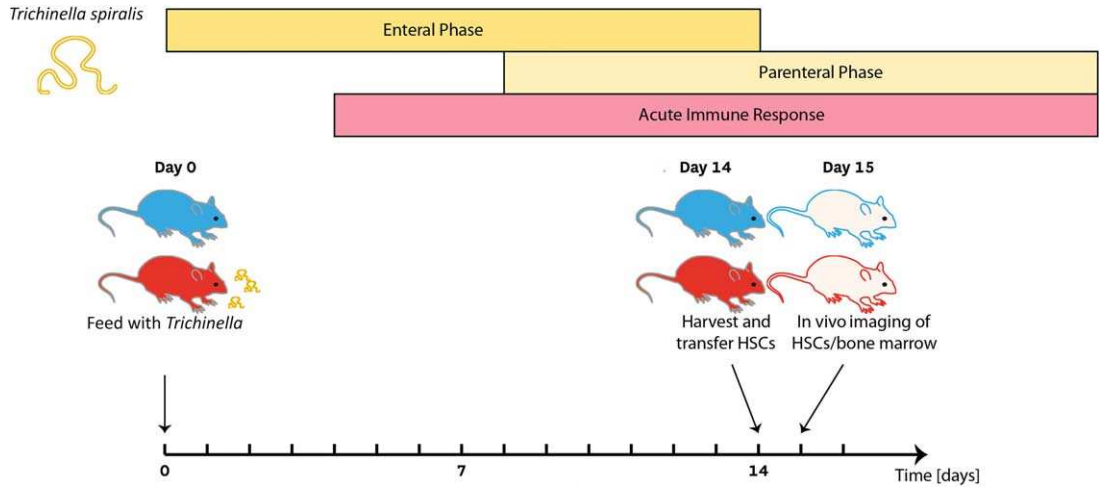


**Figure 1.** Experimental setup for studying of chronic infection. On day 0, mice are infected by oral gavage (500 larvae each). On day 14, cells are harvested from infected mice and healthy controls and sorted to obtain a population of hematopoietic stem cells. These cells are injected into lethally irradiated healthy recipients, and imaging is performed the following day. Abbreviation: HSC, hematopoietic stem cell.

The $\alpha$-shape vertices connect to form a set of m triangles $T=\{t_1, t_2, t_3,\ldots,t_m\}$, which constitute the $\alpha$-shape surface. A single vertex $v$ is connected to a set of $n$ neighboring vertices in the $\alpha$-shape by the set of connections $C=\{c_1, c_2, c_3, \ldots, c_n\}$. The curvature $\Omega$, calculated for each triangle $\tau$ in the $\alpha$-shape, is then given by

$$\Omega_\tau=\sum_{k=1}^{3}\sum_{v_c}\omega_{v_c}^{(k)}$$

where $\omega_v$ denotes the angle formed from two edges joined at vertex $v$, $v_c$ are the set of pairs of connections in $C$ such that the resulting triangle is not in $T$, and $k$ sums over each vertex in $\tau$. This average of angles calculated for each triangle is then used for quantification and visualization of $\alpha$-shape curvature. A schematic representation of this procedure is given in Supporting Information Figure S1B.

## Cell Migration Statistics

The step length and turn angle distributions are calculated directly from the cell tracks. Volume/time and surface area/time are calculated from the $\alpha$-shapes. The straightness index is calculated by $D/L$, where $D$ is the maximum displacement and $L$ is the total path length and gives a global measure of path deviations. The sinuosity index $S$ also measures path deviation, but does so around a local region of the path, and provides better estimates of the tortuosity of an undirected random walk than straightness [42]. Sinuosity $S \propto \sigma_\theta/\mu_x$, where $\sigma_\theta$ is the standard deviation of the turn angle distribution and $\mu_x$ is the mean step length. Finally, we measure the asphericity of a path by calculating the radius of gyration tensor $\bar{T}$ and defining (in 3D) the asphericity $A$ as

$$A=\frac{3\sum_{i=1}^{3}R_i^2-\left[\sum_{i=1}^{3}R_i\right]^2}{2\left[\sum_{i=1}^{3}R_i\right]^2}$$

where $R_i$s are the eigenvalues of $\bar{T}$.

## Random Walk Modeling and Inference

We use a persistent random walk model to describe stem cell migration [24, 43]. The model consists of $N$ non-interacting particles migrating in 2D. The direction of a particle's movement at any time step $t$ is described by two random variables, step length $s_t$, and turning angle $\theta_t$. A lognormal distribution is used from which to sample step lengths for each particle. The parameters of the lognormal distribution are estimated from the data separately for the control and infected groups.

The turning angle $\theta_t$ is defined without loss of generality as the angle between two consecutive motion vectors at time $t$. $\theta_t$ follows the wrapped normal distributions [44] with probability density function

$$N_w(\theta_t|\mu,\sigma)=\frac{1}{\sigma\sqrt{2\pi}}\sum_{i=0}^{\infty}\exp\left(-\frac{(\theta_t-\mu+2\pi i)^2}{2\sigma^2}\right).$$

The mean $\mu$ is 0, while the variance $\sigma$ depends on whether or not the random walker follows persistent motion. The variance for persistent motion is $\sigma_p=-2\log(p)$, with persistence parameter $p\in[0,1]$. The closer $p$ is to 1, the smaller the variances will be, and the more likely the particle will be to sample an angle 0, that is, continue in the direction of the previous step. If $p=0$, then the corresponding variance will tend to infinity and the distribution is a wrapped uniform distribution: the cell will exhibit no persistence. At each time point, $\theta_t$ and $s_t$ are determined, and the cell moves accordingly a distance of $s_t$ in the direction defined by $\theta_t$.

From trajectory data, we infer the parameters of the persistent random walk model in a Bayesian framework for the two treatment groups. The likelihood function $L(p)$ is derived exactly [24], and we sample the posterior distribution of $p$ using a standard Markov Chain Monte Carlo (MCMC) sampler. We run 5,000 MCMC steps with the first 3,000 discarded as burn-in. We used an adaptive log-Gaussian kernel for each parameter separately with the variance equal to half the variance of all previously sampled parameter values.

To determine HSC behavior over longer time intervals than is experimentally feasible or justifiable (see Experimental

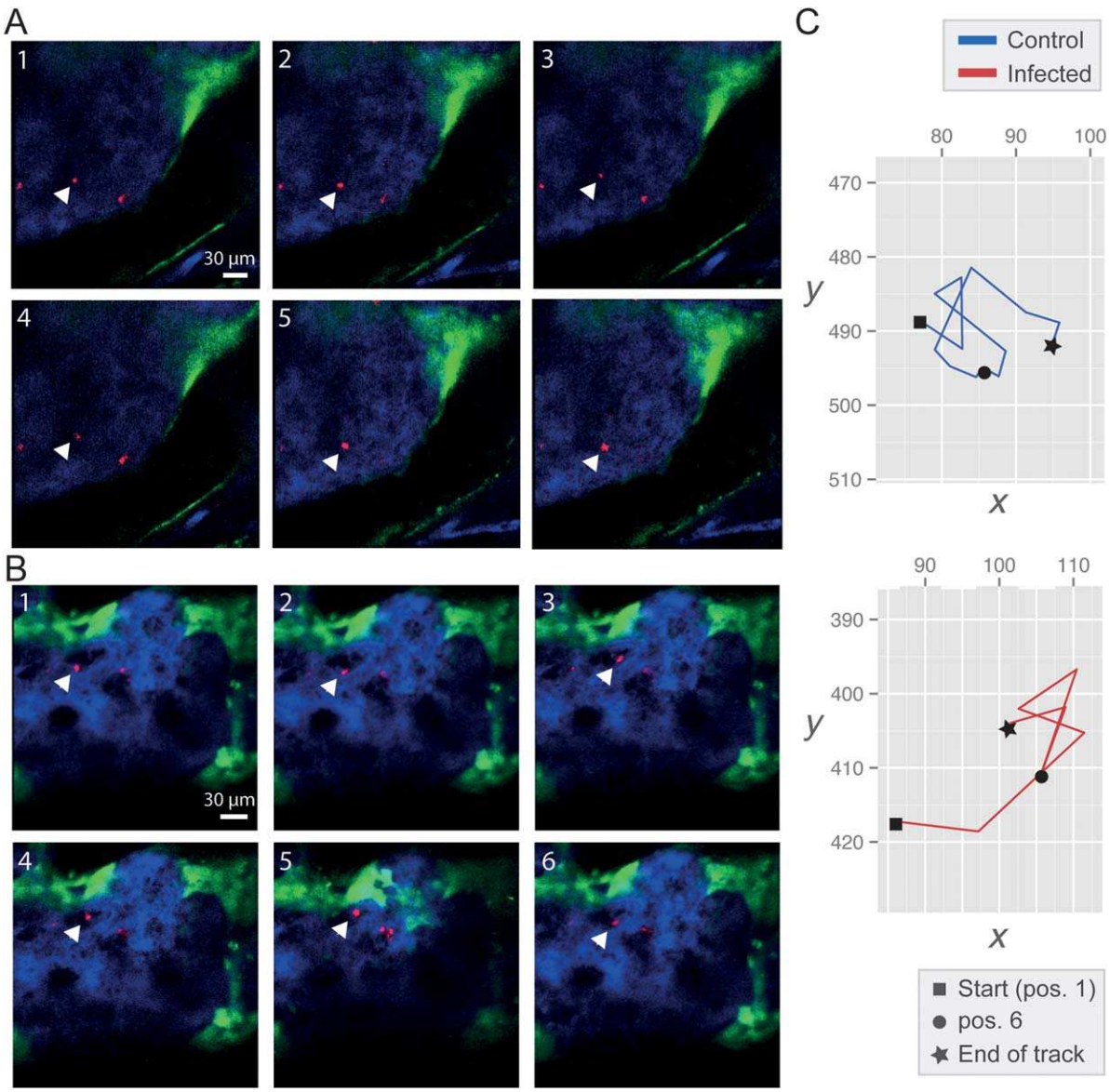


**Figure 2.** Hematopoietic stem cell (HSC) dynamics in the bone marrow microenvironment following *Trichinella* infection. **(A, B)**: Shown are the first six frames of movies that track HSCs (A) from healthy donor mice and (B) from *Trichinella*-infected mice. HSCs (red) inhabit a bone marrow niche in proximity to vasculature (blue) and osteoblasts (green). The focal cell being tracked is marked with a arrowhead. Cells were tracked over 5 hours with an interval between frames of 5 minutes; scale bar = 30 μm. **(C)**: Full-length HSC tracks corresponding to movies (A, B) projected from 3D into the *x*–*y* plane. Grid positions (in micrometer) are given relative to the imaging window. In total, 26 HSCs from infected mice and 16 HSCs from control mice were analyzed. Abbreviation: pos, position.

Design and Analysis section), we simulate 50 trajectories based on the inferred posterior distribution of the persistence and the estimated step length distributions for each group. All simulations were run for 400 time points, corresponding to 33.3 hours, starting from the origin.

## Experimental Design and Analysis

Guidelines demand that we minimize the number of experiments in animals to a level where statements of statistical significance can be made. Often a better analysis and improved experimental design can vastly increase our power to discern different types of behavior (at the same effect size), as we demonstrate here.

For the analysis of cell migration behavior, we can use this to both reduce the number of animals studied, and refine the procedure by developing better statistical analyses that allow us to identify patterns reliably in a shorter imaging window. Analysis of cell migration data is naturally simpler the longer we can track cells; different modes of cell migratory behavior can be discerned much more readily from data that contain a large number of long cell trajectories. Here, to minimize observation time, we have focused on those aspects of cell tracks that allow us to discriminate between different types of behavior but that do not require a global characterization of the paths of the cells (Supporting Information Table S1). For these measures, the collected data are sufficient to contrast the behavior of cell migration of HSCs taken from

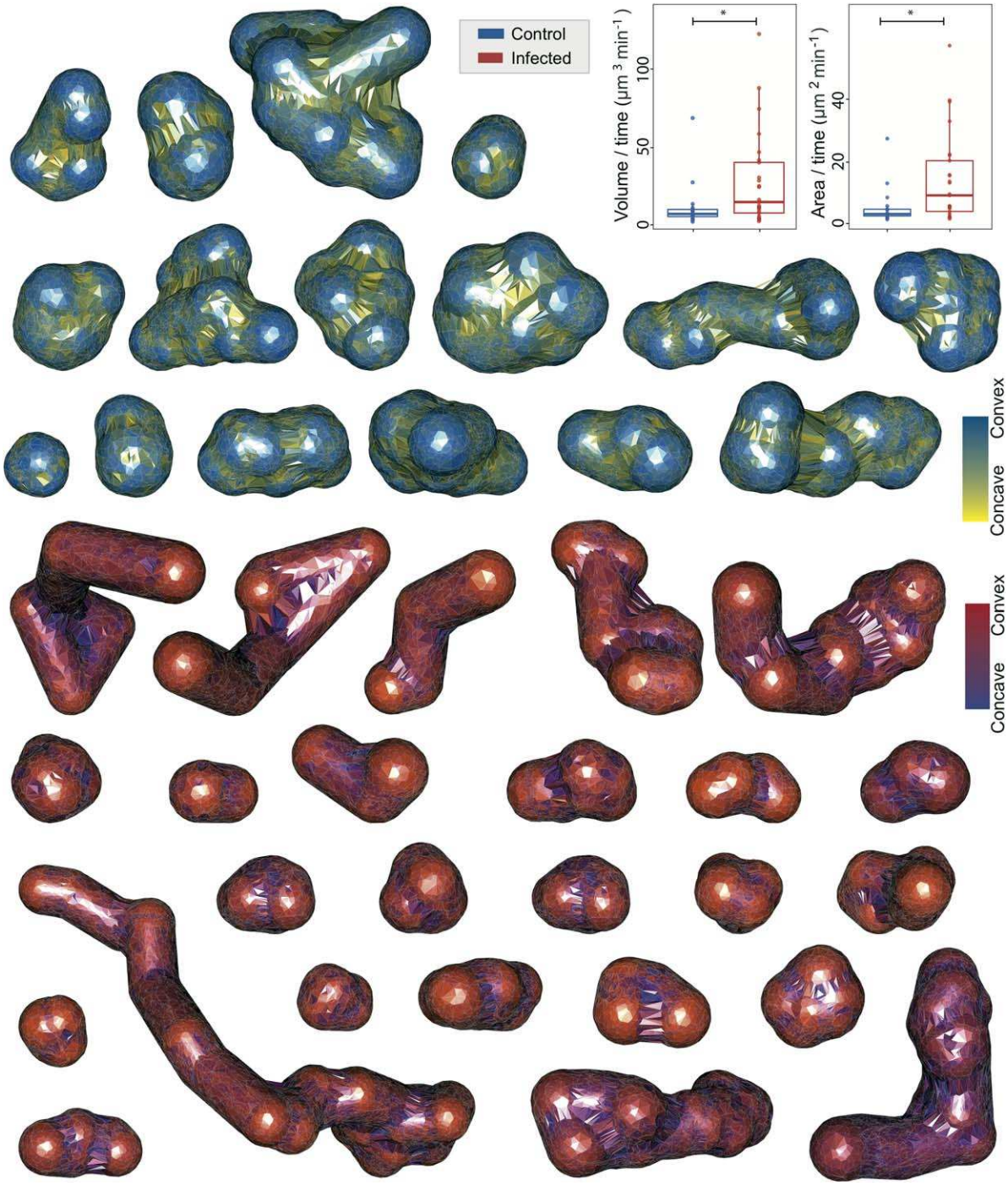


**Figure 3.** The volumes mapped out by the migration of hematopoietic stem cells (HSCs) via α-shape construction. HSCs originate from either healthy control mice ($n = 16$, blue) or *Trichinella*-infected mice ($n = 26$, red). The cells originate from the pooled calvaria of three mice from each category. Infection leads to significant changes in HSC migration behavior: HSCs are either stationary (or nearly stationary) or become highly migratory. By contrast, HSCs from uninfected mice explore a confined and stable volume within the bone marrow. The inset shows box and dot plots depicting the areas and volumes traversed by the HSCs from infected and control mice. *, $p < .05$, according to a Kolmogorov–Smirnov test.

control and infected mice and to highlight statistically significant differences between the two groups.

In addition, we performed calculations of statistical power to estimate the sample sizes that would be required to observe statistical significance for the effects seen in other migratory statistics analyzed. For the step length distribution, approximately 59 cells of each group would be required to show that the mean is different between control and infected cells, and for the turn angle, the equivalent group sample size is 98. We note that we are testing the null hypothesis of equal means—rather than equal distributions here—and also we are assuming that the variance is known and equal

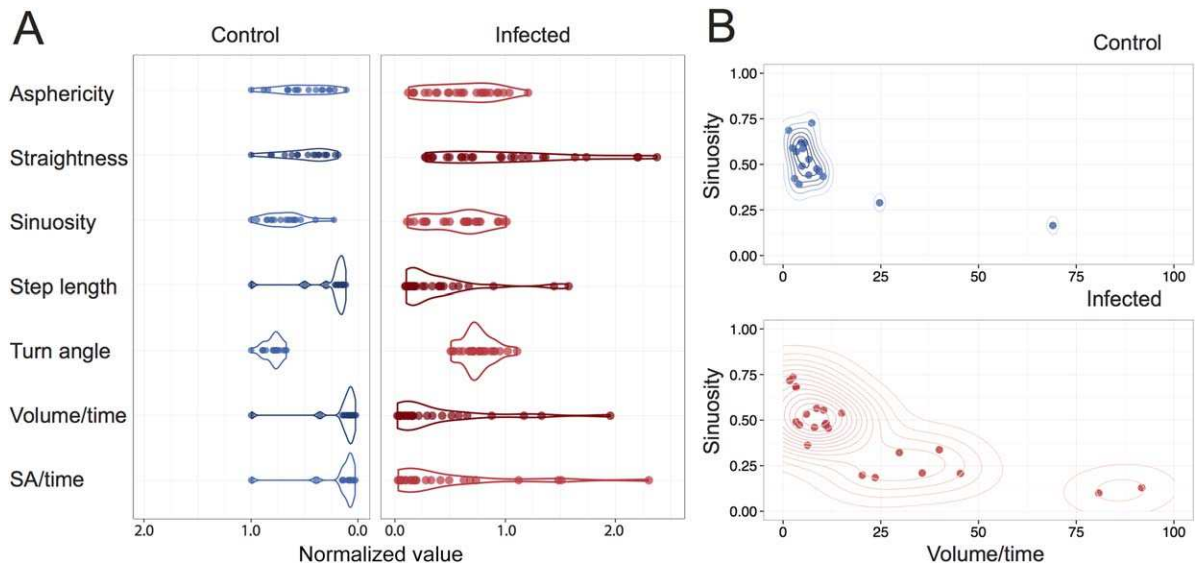


**Figure 4.** Comparison of cell migration behavior between control ($n = 16$) and *Trichinella*-infected ($n = 26$) hematopoietic stem cells. **(A)**: Migratory behaviors are studied via statistics that summarize various aspects of cell movement. For each statistic, the data are scaled by the maximum value from the healthy group; scatterplots with overlaid violin plots of the scatter density are shown. Violin plots are similar to box plots but go further in that they also show the probability density of the data at each point. Step length, volume per unit time, and surface area per unit time are significantly different between the groups ($p < .05$, Kolmogorov–Smirnov test). **(B)**: The joint density plot of two cell-track descriptors that each capture local properties of the track. Abbreviation: SA, surface area.

between groups, an assumption that may need further consideration.

## Results

### Classifying the Migratory Behavior of Individual HSCs

*Trichinella spiralis* infection provides a model with which to study the variability in responses of individual HSCs. The experimental setup is shown in Figure 1. HSCs are harvested from healthy control or day 14 infected mice, DiD-labeled, and injected into lethally irradiated recipient mice. In vivo imaging is performed approximately 16 hours later for a period of 5 hours. In Figure 2A, 2B, representative snapshots from the collected movies are shown, together with their corresponding cell tracks given in Figure 2C.

To analyze the behavior of individual HSCs in vivo, we reconstruct their 3D migration tracks; rather than using just the centre-of-mass trajectories, we use so-called $\alpha$-shapes (see Materials and Methods section), which allows us to look at the volumes traversed by HSCs (Supporting Information Fig. S1). We analyzed all cells that are found to lie within a total volume of $690 \times 580 \times 170\ \mu m^3$ inside the bone marrow cavity of the mouse calvarium. The 2D projections of the HSC tracks are shown in Supporting Information Figure S2. We study the displacement in each dimension to quantify the extent of influence of the *z*-direction on cell behavior; the variance in this direction is not significantly different from the variance in *x* or *y* (Supporting Information Fig. S2).

In Figure 3, we show the trajectories (captured by the $\alpha$-shapes) for individual infected and control HSC tracks. The $\alpha$-shape hues reflect the local average curvatures. This enables identification of their convex and concave regions, and thus allows better comparison between the trajectories and the cell behaviors. A convex region indicates that the cell visits its vicinity, partly doubling back on its path; concave curvature, by contrast, suggests forward momentum (or persistence). Here, we do find some differences: while we do not find significant differences in concavity (the total proportion of concave regions) between trajectories of HSCs harvested from infected and control mice, we find that $\alpha$-shape surfaces of HSC cells that come from infected mice show fewer transitions between concave and convex regions. This indicates that these surfaces are smoother—either rounder or more elongated—than the $\alpha$-shape surfaces of cells from non-infected mice. This, as may be gleaned from visual inspection of the trajectories in Figure 3, suggests that the "infected" HSCs either remain local (and very constrained) or exhibit "Wanderlust," a pronounced tendency to explore the bone marrow more widely, in search of a different microenvironment. $\alpha$-shapes constructed from infected cells show a significantly different distribution with respect to volumes and surface areas per unit time than those from uninfected cells (Fig. 3 inset).

### *Trichinella spiralis* Infection Leads to Heterogenous HSC Migration Patterns

To compare the movement patterns of HSCs from healthy versus *T. spiralis*-infected mice, we consider an extensive set of cell migration statistics [23, 24]. These are summarized in Figure 4A: each cell is represented by a point and the population behavior is additionally represented by violin plots (an extension of the box plot). Asphericity, straightness, and sinuosity, each characterize ways in which a track deviates from random (Brownian) motion or from a straight line [42, 45] (Supporting Information Table S1 for full definitions). We compare these statistics between control and infected cells; no significant differences are found. Straightness and sinuosity can both be used to estimate the tortuosity—or "twistedness"—of a path,

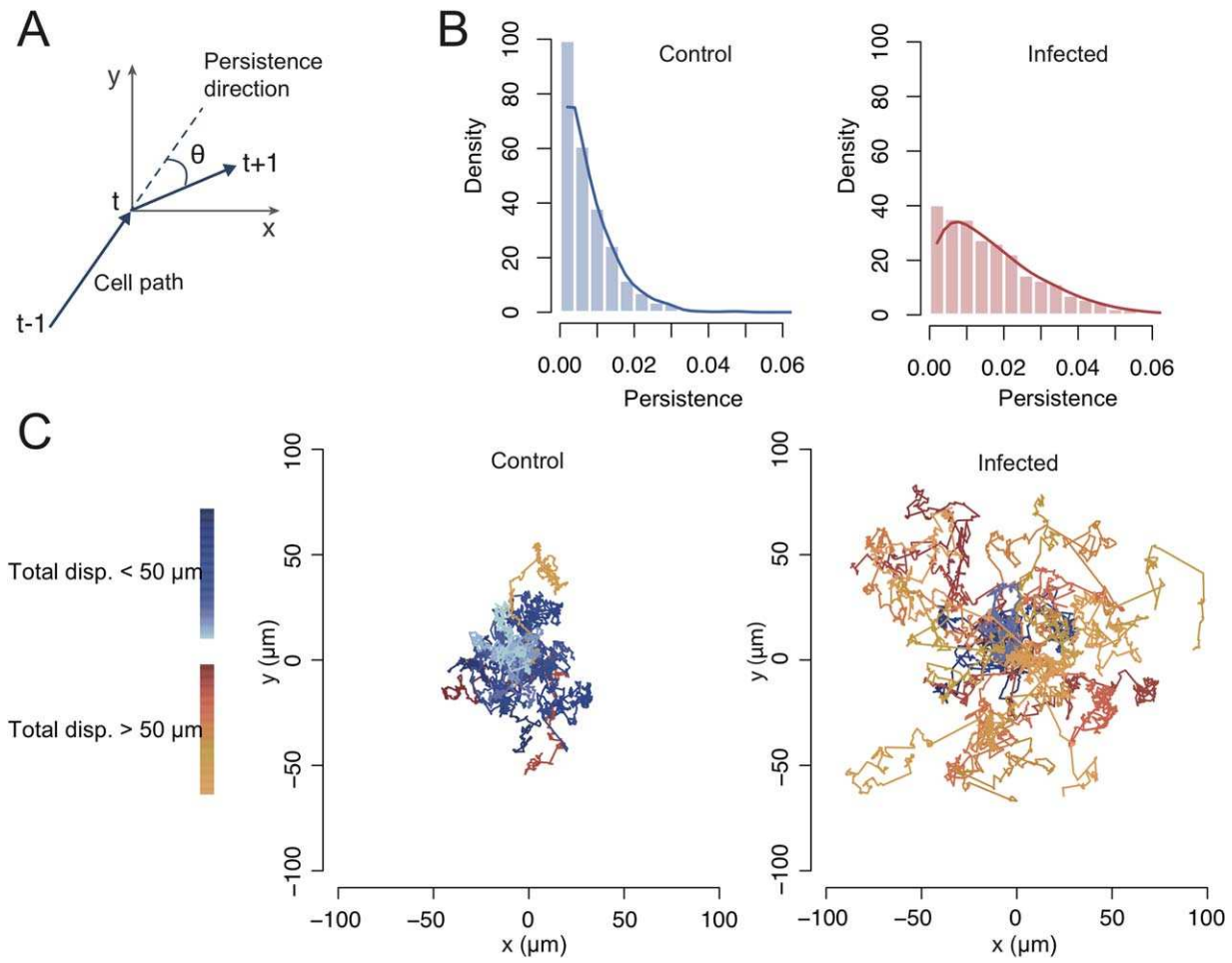


**Figure 5.** *Trichinella*-infected hematopoietic stem cells (HSCs) are more persistent than control HSCs and explore greater territories. **(A)**: Schematic description of the random walk model: a walk is simulated in 2D via sampling a step length and a persistence angle θ that quantifies a cell's deviation from a straight-line path. **(B)**: The inferred level of persistence following statistical inference that combines model and data. **(C)**: Simulations for each group from the inferred model. Each set of simulations contains 20 cell tracks of length 400 steps. Abbreviation: disp., displacement.

which can be thought of as the influence of the surroundings on one's path (e.g., physical geography on the meanders in a river). The *straightness* of a track (its total displacement/total path length) provides only a cruder estimate of tortuosity (crucially, it only becomes an appropriate statistic for classifying tracks when these get long; so it is not an optimal measure for experiments carried out in animals, where care has to be taken to limit experimental procedures to what is absolutely necessary); since it characterizes global straightness and does not account for local differences along the track; *sinuosity* is in general a better estimate of a path's tortuosity, as it characterizes local variation along sections of the track (see ref. [42] for a further details).

The distributions of step length and turn angle show no differences between control and infected cell tracks; but since there is considerable within-track variation for these statistics, this is hardly surprising. In Figure 5A, we also show the normalized values for the *volume* and *surface area* traversed by each cell per unit time; as reported (Fig. 3), we find statistically significant differences between the distributions of control and infected cells. Here, the violin plots help to illustrate both the differences in mean and in variance between the distributions.

In Figure 5B, we plot the sinuosity (twistedness) of each cell's path against the rate at which the cell explores new space (i.e., the volume per unit time). This plot highlights that cells harvested from infected mice show considerably greater variance in each statistic plotted; thus, exhibiting a greater range of behaviors than cells from control mice. Comparing the two panels of Figure 4B suggests that the HSCs collected from infected mice fall into two groups: one, which has the same characteristics as the cells from control mice (high sinuosity and low volume/time), and a second, more dispersed group with lower overall, a lower mean value for sinuosity, but a higher mean value for the volume/time. This latter group is much more mobile and migratory in behavior than the former.

### *Trichinella spiralis* Infection Leads to More Persistent Cell Movement

Random walk models describe movement (i.e., a path through space) as a sequence of steps and rotations, with, in general,

variable step lengths and turning angles. A pure random walk (also known as Brownian motion) is isotropic and displays no overall preference for direction. Other types of random walk are anisotropic by the introduction of bias (a propensity for traveling in a certain direction) or persistence (a propensity for maintaining the direction set by the previous step); models have been developed to describe cell movement in terms of these processes, such as during an immune response [24, 43].

A schematic overview of the model we introduce to study persistence, depicting two steps centered at time *t*, is shown in Figure 5A. We do not study bias here as we cannot (yet) resolve the niche-mediated signals with sufficient spatial resolution to be able to locate them. Thus, we assess the contribution of persistence to HSC movement patterns with a random walk model. The level of persistence is inferred by simulation (using MCMC, see details in Materials and Methods section). Figure 5B shows the inferred persistence distributions for cells from each group. The level of persistence for each group is small, but the persistence values for HSCs from infected mice are significantly higher overall than those for cells from non-infected mice.

Given the distributions for HSC persistence that we have inferred, we can study the behavior of HSCs by simulating their movement over time frames that are longer than are experimentally viable to capture. In Figure 5C, we simulate 20 cell tracks for each group by sampling persistence angles from the inferred posterior persistence distributions. We sample step lengths from the empirical distributions of step lengths obtained from tracking data. While we can only track cells in vivo for a period of approximately 5 hours, here we plot the tracks obtained over a simulation period of 33 hours (400 steps), to study the longer-term behavior of these cells. Figure 5C shows that the relatively small differences in persistence seen between the two groups translates into large cumulative differences in cell migration behavior over a time frame of around 1.5 days. The distances covered by the cells from the infected group mean that they have the opportunity to encounter, explore, and interact with many more potential niche cells than the non-infected HSCs.

## HSCs Perturbed by *T. spiralis* Infection Display Bimodal Behavioral Patterns

The trajectories shown in Figure 3 suggest considerable variability in migration behavior among HSCs collected from *T. spiralis*-infected mice. Particularly, they suggest bimodal behavior, whereby HSCs either occupy confined volumes, perhaps associated with particular niches, with little to no movement; or they become highly migratory and cover large spaces within the bone marrow over the course of the imaging.

To investigate this further, we analyze the dynamics exhibited by cells along their trajectories. Again, we can make use of the additional information that the $\alpha$-shapes provide and we consider how the cumulative $\alpha$-shapes are generated (Fig. 6A, 6B). "Domiciliary" cells that are constrained to stay within a limited space (perhaps due to niche supporting factors, or some other, still to be resolved physical limitations) will have a cumulative volume curve with a positive, decreasing gradient that will asymptotically approach 0 because these cells cease to continue to explore new space over time. "Exploratory" cells that are able to move more freely through space because of fewer constraints, attractant cues, or random search behavior will have a cumulative volume profile that continues to increase over time.

In Figure 6C, the cumulative volume profiles for healthy and infected HSC paths are shown. HSCs from control mice show predominantly the first pattern whereby cells are domiciliary and remain contained within a given volume. In contrast, HSCs from infected mice exhibit two patterns: one group follows the pattern of the healthy cells, maintaining domiciliary tracks, which corroborate what was seen in Figure 3, where we discern a group of cells that occupy tightly constrained volumes. The second group of cells displays markedly different behavior: these exploratory cells continue to traverse through new space over the course of the tracking period, which leads to the continuing growth of their cumulative volumes.

The relatively homogeneous movement profiles of control HSCs suggest that, at time of imaging (16 hours post transplantation), they are engaged in stable interactions with a stem cell niche within the bone marrow microenvironment. The heterogeneity of behavior seen among the cells collected from infected mice suggests some ongoing disruption of the ability to form stable HSC–niche interactions; in other words, infection may have acted to aggravate HSCs, which can no longer engage with niches as successfully. Furthermore, the data suggest that such disruption may occur as follows: in response to the disengagement of HSCs with certain niche factors, the cells adopt either a "cling-on" strategy whereby they do not move away from their current position, or a "abandon ship" strategy that causes them to travel, in search of niche engagement elsewhere.

## Decision of an HSC to Migrate from a Niche Can Be Understood in Terms of Its Life History

We can draw on life history theory to map out when it makes sense for HSCs to become mobile in the bone marrow following an infection (or other perturbation that affects the supportive relationship between a niche microenvironment in the bone marrow and hematopoietic stem cells). Life history theory describes how evolutionary forces shape functional and behavioral aspects of an organism [33, 46]. It also provides a framework in which we can study phenotypes from an evolutionary perspective, to understand if and how a given behavior/phenotype may affect an organism's long-term reproductive potential, that is, its Darwinian fitness [33]. In addition to canonical uses of life history theory, its ability to describe cellular "life" history choices has been demonstrated in application to stem cells and to cancer [47, 48].

Here, we use life history theory to study the conditions where it may become beneficial for an HSC to leave its current niche in search for a different niche microenvironment. Benefit is measured as the expected number of long-term (differentiated) offspring cells produced by an HSC adopting a given strategy, or *life-history choice* [33]. Because of the complexity of the niche, its interactions with the HSCs, and the effects of infection on the hematopoietic system, we adopt a general model that minimizes the need for making specific assumptions [49]. We assume that within a niche, $N_1$, an HSC will produce one offspring at each time step with probability *p*, the probability of division for an HSC. With probability

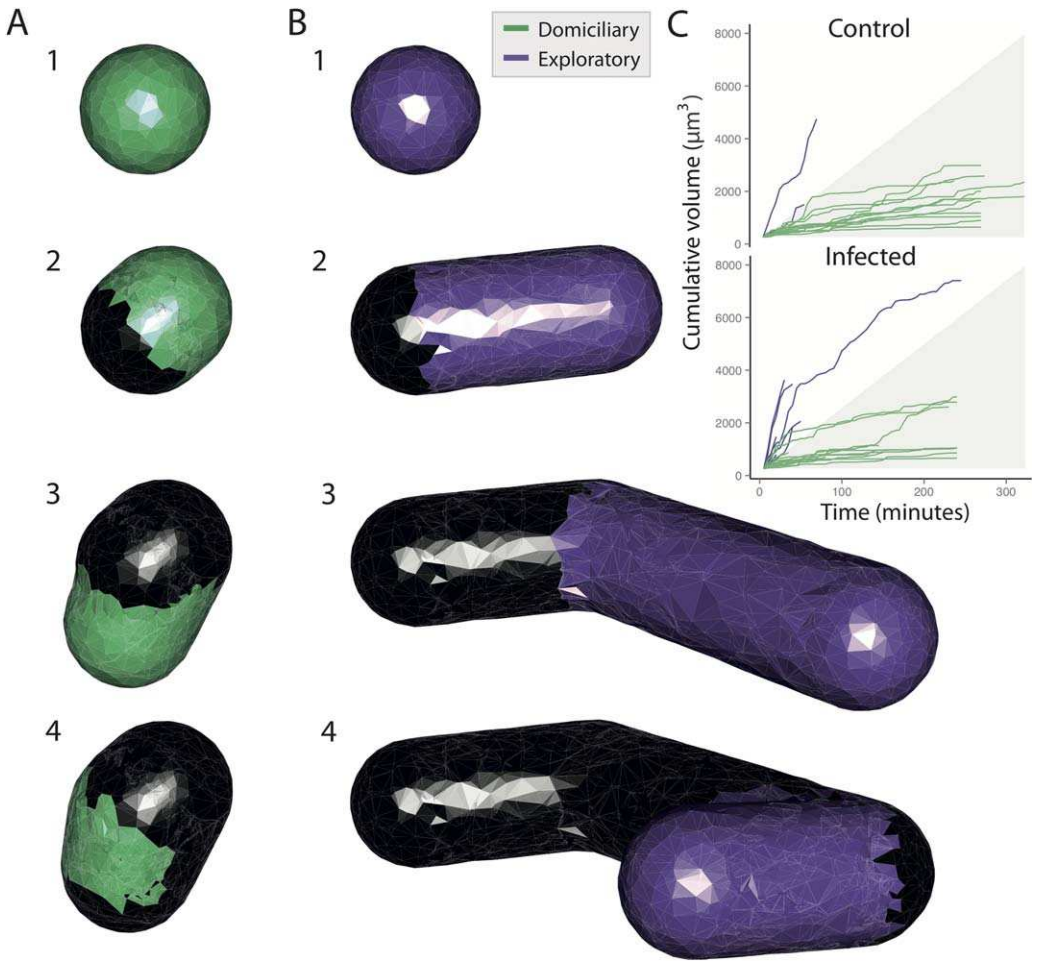


**Figure 6.** Dynamical evaluation of niche space via $\alpha$-shapes. **(A, B)**: The first four frames of two $\alpha$-shapes show their growth over time. New space visited is shown in color, and space previously occupied is shown in black. **(C)**: Trajectories of $\alpha$-shape growth depict two growth patterns: domiciliary (green) and exploratory (purple). Shaded region: [0, $\mu$ domiciliary + $\sigma$ domiciliary].

$(1-p)$, the HSC will cease producing offspring (due to loss of stemness or cell death). As we define the fitness of an HSC in terms of its ability to divide, $p$ is below referred to as a measure of the fitness of a niche. Shown in Figure 7A is a schematic representation of the relative niche fitnesses of two HSC niches and a possible path between them.

The expected number of progeny, $x$, over the lifetime of the stem cell is then

$$E[x]=\sum_{k=1}^{\infty} kp^k(1-p)=\frac{p}{1-p}, \tag{1}$$

that is, the number of differentiated cells produced is modeled as a geometric random variable. If the niche deteriorates such that the fitness is $r=\rho p$ with $0 \leq \rho \leq 1$, then we have a concomitant reduction in the expected offspring numbers, $y$, given by

$$E_\rho[y]=\frac{\rho p}{1-\rho p}. \tag{2}$$

This would be the expected number of offspring in the deteriorating niche were the HSC to stay there. If the probability of finding another functioning niche (with fitness $p$) is $\pi$, then for

$$\pi > \rho\frac{1-p}{1-\rho p}, \tag{3}$$

the expected number of offspring for a "wandering" HSC exceeds that of one that stays put in the suboptimal environment. Here, apart from the assumptions of distinct fitnesses (captured by the fitness ratio $\rho=r/p$), we have only assumed that a migrating HSC will not seek out other deteriorated niches with fitness $r$, and not move away again from a supportive niche with associated fitness $p$. These assumptions can be relaxed, but this does not, as far as we have tested, alter the qualitative behavior.

Inspection of equation (3) shows that even for relatively minor deteriorations in the HSC–niche fitness, the *mobile strategy*—that is, where the HSC becomes migratory—can become advantageous, as long as $\pi$ remains high (as shown in Fig. 7B). Prolonged insult to the bone marrow would, no doubt, lead to a decrease in $\pi$, that is, it becomes increasingly less likely to find a niche with associated high fitness, but $\rho$ also depends on the spatial location of a niche.

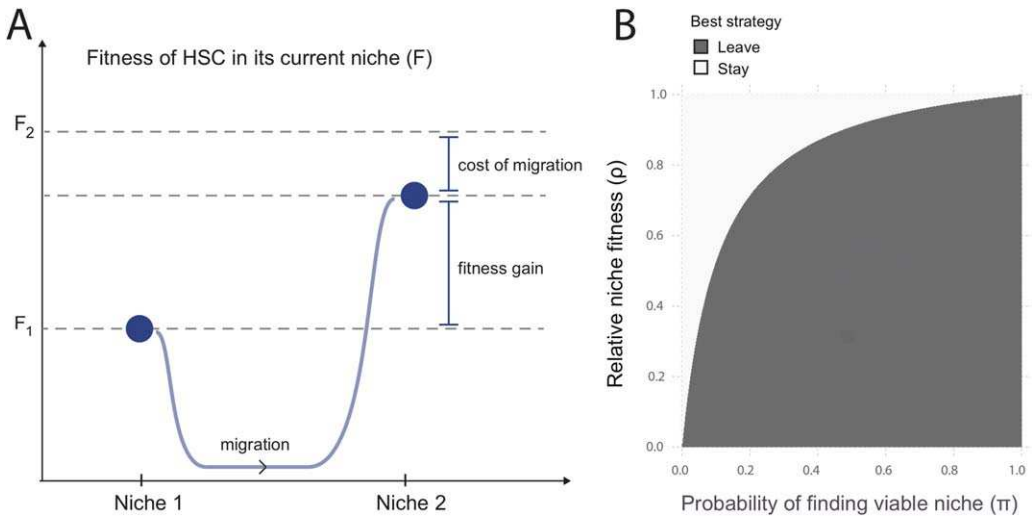


**Figure 7.** Life history trade-offs describe stem cell dynamics in the bone marrow niche. **(A)**: The blue curve denotes a possible hematopoietic stem cell trajectory between two niches N1 and N2: the best strategy is migration, as long as the cost of migration is less than the difference between niche fitnesses. **(B)**: Joint parameter space depicting the best strategy—to stay in or to leave the current niche—under different conditions. Abbreviation: HSC, hematopoietic stem cell.

In light of this analysis, the migratory phenotype is likely to be a strategy that can confer considerable advantages to the organism. Maintenance of a healthy hematopoietic system—whether it is in terms of the immune response, or the ability to oxygenate the body—is clearly important to an organism's reproductive potential. HSCs that react to an infection-driven deterioration in function by going in search of other niches would have, on average, a larger lifetime progeny potential than domiciliary HSCs that do not respond as such. We do not know at this stage whether deterioration in HSC capacity is mediated directly by infection-driven signals, or indirectly, via the niche; however we hypothesize that a niche-driven infection model may be responsible, whereby infection induces changes in the niche that are transduced via niche–stem cell interactions to HSCs. These changes are then maintained upon transplantation and drive the behavior of transplanted HSCs in new niches, at least transiently.

## Discussion

Analysis of cell behavior via tracking the migration of cells in 3D is coming of age [23, 50]. Significant progress in our understanding of cell morphology, function, and behavior has been made in recent years due to our ability to study single cells in vivo with fluorescent microscopy techniques [51–53]. Here, we have provided an in-depth investigation of the 3D migration patterns of HSCs and discovered that the stem cells exhibit a bimodal response to infection. Hematopoietic stem cells have been subject to intense scrutiny, both due to their essential role in the production of blood and as a model stem cell system [54, 55]. Nonetheless—and at least in parts due to the technical difficulties of imaging HSCs inside the bone marrow—studies that directly visualize HSCs in vivo and over time remain rare, despite the insights that they provide [21, 22, 56].

There is thus little precedent for studying HSC migration and cell movement patterns; this is especially true for the interplay between niche and HSC in cases of physiological stresses on the niche or the hematopoietic system. Previously, in ref. [22], an in vivo study of stem and progenitor cells, no movement of these cells was observed. Here, elaborating on the results of [21], we show that infection by *T. spiralis* does affect the movement patterns of individual HSCs quite considerably.

Infection affects the hematopoietic system and HSCs, in particular, in both acute and chronic disease. For chronic infections in particular, long-term morbidity due to changes to the cell population of the blood and immune system are amply documented for a range of different infectious diseases. As has been demonstrated [21], the effects of *T. spiralis* infection manifest themselves at the level of HSCs. Here, we have analyzed this behavior in more detail and have quantitatively characterized and contrasted the migration patterns of HSCs from infected and uninfected mice.

We base our analysis on the reconstructed trajectories of HSCs (using the $\alpha$-shape approach to describe the 3D trajectory of each imaged HSC) and make use of appropriate statistical descriptors of these cell tracks to capture the details of their behavior. Two central results emerge from this: HSCs collected from control mice show a uniform, largely stationary behavior. By contrast, HSCs collected from infected mice show what is essentially a bimodal behavior. Some cells remain stationary and highly localized; the remaining HSCs, however, appear to have entered an "agitated" state, which is reflected by them exploring considerable volumes compared to domiciliary HSCs.

A simple and consistent (but almost certainly not the only possible) explanation is that this behavior reflects a deterioration of the HSC–niche relationship in the infected mice. In such circumstances, changes to the stem cell may impede its ability to interact with the current niche as is required to maintain its function. Subsequently, an HSC may become

agitated enough to move away from the niche. This may either be an active process to find an alternative niche environment; or a passive process, if, for example, a niche-retaining signal is lost because of deterioration in the stem cell–niche relationship.

Hematopoietic stem cells must make choices about the migratory behavior they adopt in a manner similar to the way in which they make choices about division and cell fate [57–59]. It seems natural, therefore, to consider the migration behavior of HSCs (and perhaps also myeloid and lymphoid progenitors [60]) as a response to stress in or near to the niche, as well as perhaps a response to a deteriorating niche. Given the characterization of HSC migration patterns in the bone marrow, a pressing question regards why these stem cells follow the particular movement patterns observed. But our mathematical analysis—building on a large body of work in life history theory—also highlights the distinct possibility that such migration behavior could be an adaptive, evolutionarily favorable response. As we have shown above for a very parsimonious (as far as possible assumption-free) model of stem cell fate, an HSC that actively leaves a niche in search of a more supportive microenvironment may—under a wide range of scenarios—increase its long-term number of progeny. In other words, if there is a high chance of finding a niche for which a cell is better suited, the proclivity of HSCs to leave their niche should be very high. Most interestingly, and as expected based on our model, we have previously shown that HSCs from *T. spiralis* infected animals have an advantage in reconstituting irradiated recipient mice, as shown by long-term increased engraftment in a competitive bone marrow transplantation setting [21].

In the same vein, we can also start to consider the heterogeneity exhibited by HSCs that have been exposed to infection: biological heterogeneity has strong links to robustness. Given the uncertainty of many environments and the change in demands on an organism, these may provoke, using heterogeneous phenotypes in response appears to be a strategy that has been repeated throughout nature across multiple biological scales [61–63]. Even the existence of certain intermediate progenitor populations has recently been called into question as the role of heterogeneity in the hematopoietic hierarchy grows [64, 65]. Our data suggest that the ability of stem cells to respond to a perturbation mediated via infection is founded in part upon the heterogeneity present in the HSC pool within bone marrow.

We can extend these arguments further and explore the predictions that this model makes. These include: (a) upon infection, we would expect to see depletion of niches that are most easily exposed to a pathogen. (b) Some HSCs may even for prolonged infection leave the bone marrow and enter the blood stream.

We would expect that these effects will differ between different infectious diseases, their etiology, the inflammatory response they elicit, and the way in which their effects manifest themselves among the cells that make up the niche. The effects are also almost certainly not limited to infectious diseases. For example, from ref. 66, it was found that periarteriolar niche cells are lost in acute myelogeneous leukemia-induced sympathetic neuropathy. Or, as another example, Interleukin 27 is an inflammatory marker that has been implicated in changing the size and behavior of the HSC pool [67]. These lines of evidence are perfectly in line with the first prediction. The second implication of our results is in good agreement with well-established observations that show an increased level of hematopoiesis (also increased numbers of detectable HSCs) in secondary sites of adult hematopoiesis—in particular the spleen—following infection [27]: whereas, these sites normally appear to harbor few (if any) HSCs, during infection, HSC activity in the spleen increases considerably, although it is difficult to determine whether these HSCs migrated directly from the bone marrow. We note that the notion of migratory behavior as an evolutionary favorable strategy has also recently been suggested in ecological settings [68].

This study was able to demonstrate and characterize quantitatively the range of different in vivo behaviors of HSCs that have been exposed to an infection, and to contrast this with HSCs collected from control mice. Based on the life history analysis, we suggest that the variability in mobility among HSCs collected from infected mice could represent an adaptation and may thus be actively maintained. How inflammatory signals are received and processes by HSCs and/or niche maintaining cells is incompletely understood. Extracting phenotypic data (such as here) and molecular information/profiles (transcriptomic/proteomic) simultaneously is currently not possible. In any case, detecting variability at the transcriptional and/or proteomic level between HSCs will require vast numbers of cells, prohibitively so, for in vivo experiments in suitable model systems, such as for murine hematopoiesis.

The lack of a meaningful in vitro system where such phenomena could be dissected in more detail is both vexing, and—almost certainly—a hallmark of the stem cell's dependence on its supporting microenvironment. Phenotyping via imaging must be done in vivo: the 3D structure of the bone marrow and the complex set of interactions between the niche-maintaining cells/factors crucially affect the behavior of HSCs, and their response to infection or other perturbations. What may help is an in silico niche that allows us to explore how different mechanistic assumptions or hypotheses affect HSC behavior. Not only would this allow us to place our in vivo phenotyping data in the context of available mechanistic knowledge, as well as assumptions, but it would also allow us to make use of modern, simulation-based approaches of experimental design.

## Conclusion

Hematopoietic stem cells reside in the bone marrow where they are crucially maintained by an incompletely characterized set of niche factors. Recently it has been shown that chronic infection profoundly affects hematopoiesis by exhausting stem cell function, but these changes have not yet been resolved at the single cell level. Here, we show that the stem cell–niche interactions triggered by infection are heterogeneous whereby cells exhibit different behavioral patterns: for some, movement is highly restricted, while others explore much larger regions of space over time. Overall, cells from infected mice display higher levels of persistence. This can be thought of as a search strategy: during infection the signals passed between stem cells and the niche may be blocked or inhibited. Resultantly, stem cells must choose to either "cling on,"

or to leave in search of a better environment. The heterogeneity that these cells display has immediate consequences for translational therapies involving bone marrow transplant, and the effects that infection might have on these procedures.

## Acknowledgments

We thank Marc Mangel for comments on the manuscript. This work was supported by the Biotechnology and Biological Sciences Research Council (BB/L023776/1) (to A.L.M., R.K., C.L.C., and M.P.H.S.) and the National Centre for the Replacement, Refinement and Reduction of Animals in Research (NC/K001949/1) (to J.L.). A.L.M. is currently affiliated with the Department of Mathematics, University of California, Irvine, CA; M.A.S. is currently affiliated with the Department of Molecular Oncology, BC Cancer Agency, and Graduate Bioinformatics Training Program, University of British Columbia Vancouver, BC, Canada; J.L. is currently affiliated with the Max Planck Institute for Biophysical Chemistry, Göttingen, Germany; N.S. is currently affiliated with the Max Planck Institute of Molecular Cell Biology and Genetics Dresden, Germany.

## Author Contributions

A.L.M., C.L.C. and M.P.H.S. conceived the study; A.L.M., M.A.S., J.L. & A.S. analyzed the data; R.K., N.M.R., N.S., A.K., I.R. provided data and additional analysis; A.L.M. & M.P.H.S. conducted the mathematical analysis; A.L.M., M.A.S., C.L.C. and M.P.H.S. wrote the manuscript. All authors saw and approved the final manuscript.

## Disclosure of Potential Conflicts of Interest

The authors indicated no potential conflicts of interest.

## References

**1** Orkin SH, Zon LI. Hematopoiesis: An evolving paradigm for stem cell biology. Cell 2008;132:631–644.
**2** Durand EM, Zon LI. Stem cells: The blood balance. Nature 2010;468:644–645.
**3** Ding L, Saunders TL, Enikolopov G et al. Endothelial and perivascular cells maintain haematopoietic stem cells. Nature 2012;481:457–462.
**4** Schütte J, Wang H, Antoniou S et al. An experimentally validated network of nine haematopoietic transcription factors reveals mechanisms of cell state stability. eLife 2016;5:e11469.
**5** Morrison SJ, Scadden DT. The bone marrow niche for haematopoietic stem cells. Nature 2014;505:327–334.
**6** Boulais PE, Frenette PS. Making sense of hematopoietic stem cell niches. Blood 2015;125:2621–2629.
**7** Acar M, Kocherlakota KS, Murphy MM et al. Deep imaging of bone marrow shows non-dividing stem cells are mainly perisinusoidal. Nature 2015;526:126–130.
**8** Bowers M, Zhang B, Ho Y et al. Osteoblast ablation reduces normal long-term hematopoietic stem cell self-renewal but accelerates leukemia development. Blood 2015;125:2678–2688.
**9** Itkin T, Gur-Cohen S, Spencer JA et al. Distinct bone marrow blood vessels differentially regulate haematopoiesis. Nature 2016;532:323–328.
**10** Kusumbe AP, Ramasamy SK, Itkin T et al. Age-dependent modulation of vascular niches for haematopoietic stem cells. Nature 2016;532:380–384.
**11** Sugiyama T, Kohara H, Noda M et al. Maintenance of the hematopoietic stem cell pool by CXCL12-CXCR4 chemokine signaling in bone marrow stromal cell niches. Immunity 2006;25:977–988.
**12** Méndez-Ferrer S, Michurina TV, Ferraro F et al. Mesenchymal and haematopoietic stem cells form a unique bone marrow niche. Nature 2010;466:829–834.
**13** Calvi LM, Adams GB, Weibrecht KW et al. Osteoblastic cells regulate the haematopoietic stem cell niche. Nature 2003;425:841–846.
**14** Sipkins DA, Wei X, Wu JW et al. In vivo imaging of specialized bone marrow endothelial microdomains for tumour engraftment. Nature 2005;435:969–973.
**15** Adams GB, Chabner KT, Alley IR et al. Stem cell engraftment at the endosteal niche is specified by the calcium-sensing receptor. Nature 2006;439:599–603.
**16** Kiel MJ, Yilmaz OH, Iwashita T et al. SLAM family receptors distinguish hematopoietic stem and progenitor cells and reveal endothelial niches for stem cells. Cell 2005;121:1109–1121.
**17** Lo Celso C, Fleming HE, Wu JW et al. Live-animal tracking of individual haematopoietic stem/progenitor cells in their niche. Nature 2009;457:92–96.
**18** Nombela-Arrieta C, Pivarnik G, Winkel B et al. Quantitative imaging of haematopoietic stem and progenitor cell localization and hypoxic status in the bone marrow microenvironment. Nat Cell Biol 2013;15:533–543.
**19** Kylafis G, Loreau M. Niche construction in the light of niche theory. Ecol Lett 2011;14:82–90.
**20** Tamplin OJ, Durand EM, Carr LA et al. Hematopoietic stem cell arrival triggers dynamic remodeling of the perivascular niche. Cell 2015;160:241–252.
**21** Rashidi NM, Scott MK, Scherf N et al. In vivo time-lapse imaging shows diverse niche engagement by quiescent and naturally activated hematopoietic stem cells. Blood 2014;124:79–83.
**22** Kohler A, Schmithorst V, Filippi M-D et al. Altered cellular dynamics and endosteal location of aged early hematopoietic progenitor cells revealed by time-lapse intravital imaging in long bones. Blood 2009;114:290–298.
**23** Masuzzo P, Van Troys M, Ampe C et al. Taking aim at moving targets in computational cell migration. Trends Cell Biol 2016;26:88–110.
**24** Jones PJM, Sim A, Taylor HB et al. Inference of random walk models to describe leukocyte migration. Phys Biol 2015;12:066001.
**25** Rodriguez S, Chora A, Goumnerov B et al. Dysfunctional expansion of hematopoietic stem cells and block of myeloid differentiation in lethal sepsis. Blood 2009;114:4064–4076.
**26** Essers MAG, Offner S, Blanco-Bose WE et al. activates dormant haematopoietic stem cells in vivo. Nature 2009;458:904–908. IFNα
**27** Baldridge MT, King KY, Boles NC et al. Quiescent haematopoietic stem cells are activated by IFN-γ in response to chronic infection. Nature 2010;465:793–797.
**28** King KY, Goodell MA. Inflammatory modulation of HSCs: Viewing the HSC as a foundation for the immune response. Nat Rev Immunol 2011;11:685–692.
**29** Cabezas Wallscheid N, Eichwald V, Graaf J. D et al. Instruction of haematopoietic lineage choices, evolution of transcriptional landscapes and cancer stem cell hierarchies derived from an AML1-ETO mouse model. EMBO Mol Med 2013;5:1804–1820.
**30** Geiger H, Haan G de, Florian MC. The ageing haematopoietic stem cell compartment. Nat Rev Immunol 2013;13:376–389.
**31** Despommier DD, Campbell WC. Synopsis of morphology. In: Campbell WC, ed. Trichinella and Trichinosis. Plenum Press, New York, NY, 1983:551–561.
**32** Beiting DP, Gagliardo LF, Hesse M et al. Coordinated control of immunity to muscle stage *Trichinella spiralis* by IL-10, regulatory T cells, and TGF-beta. J Immunol 2007;178:1039–1047.
**33** Stearns SC. The Evolution of Life Histories. Oxford University Press, Oxford, UK, 1992.
**34** Aktipis CA, Boddy AM, Gatenby RA et al. Life history trade-offs in cancer evolution. Nat Rev Cancer 2013;13:883–892.
**35** Slatkin M. Hedging one's evolutionary bets. Nature 1974;250:704–705.
**36** Stumpf MPH, Laidlaw Z, Jansen VAA. Herpes viruses hedge their bets. Proc Natl Acad Sci USA 2002;99:15234–15237.
**37** Balázsi G, Oudenaarden A van, Collins JJ. Cellular decision making and biological noise: From microbes to mammals. Cell 2011;144:910–925.
**38** Schindelin J, Arganda-Carreras I, Frise E et al. Fiji: An open-source platform for biological-image analysis. Nat Methods 2012;9:676–682.

**39** Edelsbrunner H, Mücke EP. Three-dimensional alpha shapes. ACM Trans Graph 1994; 13:43–72.

**40** Edelsbrunner H, Koehl P. The weighted-volume derivative of a space-filling diagram. Proc Natl Acad Sci USA 2003;100:2203–2208.

**41** Albou L-P, Schwarz B, Poch O et al. Defining and characterizing protein surface using alpha shapes. Proteins 2009;76:1–12.

**42** Benhamou S. How to reliably estimate the tortuosity of an animal's path: Straightness, sinuosity, or fractal dimension? J Theor Biol 2004;229:209–220.

**43** Liepe J, Taylor HB, Barnes CP et al. Calibrating spatio-temporal models of leukocyte dynamics against in vivo live-imaging data using approximate Bayesian computation. Integr Biol 2012;4:335–345.

**44** Breitberger E. Analogues of the normal distribution on the circle and the sphere. Biometrika 1963;50:81–88.

**45** Rudnick J, Gaspari G. Elements of the Random Walk. Cambridge University Press, Cambridge, UK, 2004.

**46** Gluckman P, Beedle A, Hanson M. Principles of Evolutionary Medicine. Oxford University Press, Oxford, UK, 2009.

**47** Mangel M, Bonsall MB. Phenotypic evolutionary models in stem cell biology: Replacement, quiescence, and variability. PLoS ONE 2008;3:e1591.

**48** Dingli D, Chalub FACC, Santos FC et al. Cancer phenotype as the outcome of an evolutionary game between normal and malignant cells. Br J Cancer 2009;101:1130–1136.

**49** May RM. Uses and abuses of mathematics in biology. Science 2004;303:790–793.

**50** Driscoll MK, Danuser G. Quantifying Modes of 3D Cell Migration. Trends Cell Biol 2015;25:749–759.

**51** Feng Y, Santoriello C, Mione M et al. Live imaging of innate immune cell sensing of transformed cells in zebrafish larvae: Parallels between tumor initiation and wound inflammation. PLoS Biol 2010;8:e1000562.

**52** Lo Celso C, Lin CP, Scadden DT. In vivo imaging of transplanted hematopoietic stem and progenitor cells in mouse calvarium bone marrow. Nat Prot 2011;6:1–14.

**53** Tozluoğlu M, Tournier AL, Jenkins RP et al. Matrix geometry determines optimal cancer cell migration strategy and modulates response to interventions. Nat Cell Biol 2013; 15:751–762.

**54** Enver T, Pera M, Peterson C et al. Stem cell states, fates, and the rules of attraction. Cell Stem Cell 2009;4:387–397.

**55** MacLean AL, Kirk P, Stumpf MPH. Cellular population dynamics control the robustness of the stem cell niche. Biol Open 2015; 10.1242–bio.013714.

**56** Lassailly F, Foster K, Lopez-Onieva L et al. Multimodal imaging reveals structural and functional heterogeneity in different bone marrow compartments: Functional implications on hematopoietic stem cells. Blood 2013;122:1730–1740.

**57** Wilson A, Laurenti E, Trumpp A. Balancing dormant and self-renewing hematopoietic stem cells. Curr Opin Genet Dev 2009;19:461–468.

**58** Simons BD, Clevers H. Strategies for homeostatic stem cell self-renewal in adult tissues. Cell 2011;145:851–862.

**59** Garcia-Ojalvo J, Martinez Arias A. Towards a statistical mechanics of cell fate decisions. Curr Opin Genet Dev 2012;22:619–626.

**60** Sun J, Ramos A, Chapman B et al. Clonal dynamics of native haematopoiesis. Nature 2014;514:322–327.

**61** Paszek P, Ryan S, Ashall L et al. Population robustness arising from cellular heterogeneity. Proc Natl Acad Sci USA 2010;107: 11644–11649.

**62** Satija R, Shalek AK. Heterogeneity in immune responses: From populations to single cells. Trend Immunol 2014;35:219–229.

**63** Feinerman O, Veiga J, Dorfman JR et al. Variability and robustness in T cell activation from regulated heterogeneity in protein levels. Science 2008;321:1081–1084.

**64** Paul F, Arkin Y, Giladi A et al. Transcriptional heterogeneity and lineage commitment in myeloid progenitors. Cell 2015;163: 1663–1677.

**65** Notta F, Zandi S, Takayama N et al. Distinct routes of lineage development reshape the human blood hierarchy across ontogeny. Science 2016;351:aab2116–aab2116.

**66** Hanoun M, Zhang D, Mizoguchi T et al. Acute myelogenous leukemia-induced sympathetic neuropathy promotes malignancy in an altered hematopoietic stem cell niche. Cell Stem Cell 2014;15:365–375.

**67** Furusawa J-I, Mizoguchi I, Chiba Y et al. Promotion of expansion and differentiation of hematopoietic stem cells by interleukin-27 into myeloid progenitors to control infection in emergency myelopoiesis. PLoS Path 2016; 12:e1005507.

**68** Tan ZX, Cheong KH. Nomadic-colonial life strategies enable paradoxical survival and growth despite habitat destruction. eLife 2017;6:e21673.

See www.StemCells.com for supporting information available online.